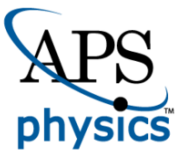

Thermal Rectification via Heterojunctions of Solid-State Phase-Change Materials

Hyungmook Kang, Fan Yang, and Jeffrey J. Urban

Phys. Rev. Applied **10**, 024034 — Published 23 August 2018

DOI: 10.1103/PhysRevApplied.10.024034

Thermal rectification via heterojunctions of solid-state phase change materials

Hyungmook Kang [1,2], Fan Yang [1] and Jeffrey J. Urban [1, *]

[1] *The Molecular Foundry, Lawrence Berkeley National Laboratory, Berkeley, California 94720, USA*
[2] *Department of Mechanical Engineering, University of California, Berkeley, California 94720, USA*
[*] Author to whom correspondence should be addressed. Electronic address: jjurban@lbl.gov

ABSTRACT

Nonlinear thermal transport can arise naturally in materials with strongly temperature-dependent thermal conductivities, however, this is exceedingly rare and weak. If a general strategy could be devised to yield nonlinear thermal transport, it would provide an avenue to controlling heat flow and realizing nonlinear thermal devices. Phase change materials, which can exist in two states with distinct thermal conductivities, provide a unique opportunity to realize nonlinear thermal transport. In this work, we develop an analytical framework upon which we propose a material architecture for actualizing one type of nonlinear thermal transport, thermal rectification, where heat flux is biased in one direction. Our findings show that a heterojunction of two tunable phase change materials can demonstrate strong thermal rectification. The magnitude of thermal rectification is analyzed as a function of the phase change properties of each material, and we determine the fundamental heat flux relations for each direction in these heterojunctions and criteria to separate the various phase situations which can occur. Finally, the analytical framework is applied to a junction comprised of two phase change materials, polyethylene and vanadium dioxide, and demonstrate a maximal theoretical rectification factor of ~140%. This analysis provides an important analytical tool in helping researchers design thermal circuits or advanced thermal energy storage media.

I. INTRODUCTION

Inspired by the conceptual keystone of the microelectronics industry, the transistor, research on thermal transport with nonlinear thermal properties, such as nonlinear temperature- (or atomic mass, pressure, geometry) dependent thermal conductivities, has attracted a great deal of attention in recent years. Thermal devices including thermal rectifiers[1-15] and thermal transistors[1, 2] have been realized by nonlinear transport phenomena such as thermal rectification (i.e. heat transport characterized by a preferential direction for heat flow, as described in Fig. 1(a)). To achieve thermal rectification, several mechanisms at solid states have been suggested, such as enhancing lattice anharmonicity,[2, 16] use of asymmetric nanostructures,[4-9] defects in structures[10, 11] and asymmetric scattering of photons.[12-14] However, none of these proposed mechanisms has yielded materials with large thermal rectification, experimentally and analytically. Another promising mechanism, solid-state junctions using phase change materials, have been recently used for thermal rectification[17-20] and show great potential for making devices that scale effectively. *Cottrill et. al.*[21] analyzed the thermal rectification in a single phase change material. However, they limited their analysis to the simplest case with only one phase change material and thus can only provide rectification defined by the contrast of the high and low thermal conductivity phase of that individual material. The parametric study to obtain the thermal rectification remained in numerical approach, without an empirical solution for the maximal performance. Recently, they extended the approach to a junction with two phase change materials, however, considered limited cases which can make only one phase change situation at one time.[22] *Ordonez-Miranda et. al.*[23] studied an added hysteresis effect of a phase change material in the junction and figured out the main key parameter for the thermal rectification is thermal conductivity contrast of the phase change material. In addition, due to the lack of choice of appropriate materials, the thermal bias spans a very broad range (>50 K), limiting its use in applications such as thermal energy storage and thermal circuits, which usually operate in a narrow thermal bias. The thermal rectification effect occurring in a narrow temperature window results in a greater potential to enhance when the thermal bias increases.

In this paper, we propose a general theory that can handle multiple phase change materials and interfaces, thus providing large thermal rectification ratios well-beyond that provided by the mere thermal conductivity contrast of any one individual material. Specifically, heterojunctions using two phase change materials can strongly

enhance the thermal rectification with the advantage of additional interfaces, as depicted in Fig. 1(b). This work encompasses a full physical picture of heat transport in phase change materials, fundamentally addressing all possible experimentally observable scenarios of thermal rectification. Then, this paper applies the general theory to real rapid jump thermal conductivity materials. With recent advancements in solid-state materials, phase transitions can occur over just a few degrees in temperature. One prominent example is the metal-insulator-transition (MIT) which occurs in tungsten doped vanadium dioxide (VO_2).[24] It has a MIT phase change in a very small temperature window (~5 K) which can show a thermal conductivity contrast clearly, and a higher thermal conductivity when the temperature rises across the MIT temperature. Thus, combining it with another material with the opposite temperature dependence, thermal rectification can be enhanced. Finally, the general theory suggests the theoretical maximum of thermal rectification factor of the solid-state junctions.

II. THEORETICAL MODEL

A. Heterojunction design

We start with a junction formed by two materials, A and B, each possessing a phase change at temperatures T_A^* and T_B^*, respectively. For bulk or thin film samples, we assume heat transfer is a one-dimensional problem. Without losing generality, we take the case where material "B" has a higher phase change temperature than "A" (i.e. $T_A^*<T_B^*$). We also assume that A has a thermal conductivity, $k_{A,L}$, at low temperature and a thermal conductivity, $k_{A,H}$, at high temperature. Here, the subscripts denote the material index and temperature region in relation to its phase change temperature (higher or lower), respectively. We also apply analogous nomenclature to material B. For simplicity, we assume thermal conductivity is a step function with respect to temperature through the phase change. This step function assumption is supported by the acceptable similarity of thermal conductivity trend in several materials within a large temperature range.[24, 25] The schematic in Fig. 1(b) represents the geometry of the junction in materials A and B of lengths l_A and l_B, respectively. We name the heat flux traveling in the direction depicted in Fig. 1(b) as q_{LH} and the heat flux traveling in the opposite direction as q_{HL}. We treat the heat flux directions separately, meaning q_{LH} and q_{HL} represent their absolute magnitude. With heat flux in both directions, we define the thermal rectification factor as the normalized heat flux difference,

$$\gamma = \frac{\max\{q_{LH}, q_{HL}\}}{\min\{q_{LH}, q_{HL}\}} - 1. \tag{1}$$

In general linear thermal transport, especially, no thermal rectification, the thermal rectification factor should be the minimum value, zero. The designed heterojunction would have a thermal rectification factor trend depending on thermal bias with an optimum, as predicted in Fig. 1(c).

B. General theory results

The governing equation for this study is Fourier's law under steady state conditions. We assume that the thermal boundary resistance at the junction is negligible. The ratio of thermal boundary resistance to the thermal resistance of materials can affect the thermal rectification factor.[22] The eligible device length depends on the thermal conductivity of the applied materials and the contact resistance at the interface between different materials. This assumption holds if the device length is on the order of 300 nm or longer, since the most of similar thermal contact conductance at interface between different materials is on the order of 100 MW/m^2K[26-28] and the minimum order of that is around 30 MW/m^2K.[29-32] The boundary conditions are the temperatures T_H and T_L and the known phase change temperatures T_A^* and T_B^*. Heat fluxes through each material or phase are described by:

$$-q = k_{A,L}\left.\frac{\partial T}{\partial x}\right|_{T<T_A^*} = k_{A,H}\left.\frac{\partial T}{\partial x}\right|_{T>T_A^*} = k_{B,L}\left.\frac{\partial T}{\partial x}\right|_{T<T_B^*} = k_{B,H}\left.\frac{\partial T}{\partial x}\right|_{T>T_B^*} \tag{2}$$

The problem we consider here is a general case with two phase change materials. When the thermal bias, T_H-T_L, changes, the phase change interface in the materials moves. There are a multitude of different factors that must be taken into consideration, such as the phase change could happen in A and/or B, or the flux direction yields different amounts of heat flux. In this study, we analytically derive the heat flux for all cases and the criteria to determine an appropriate case, compute the thermal rectification factor, γ, and give suggestions for designing an optimal thermal rectifier.

Firstly, we start from conditions that the phase change temperatures for both materials are between T_L and T_H (i.e. $T_L \le T_A^* \le T_H$ and $T_L \le T_B^* \le T_H$). Given these conditions, there are four possible cases of heat flux for the q_{LH} direction with respect to the interface position of the phase change: a phase change occurs only in material A or B, or in both or none of the materials. On the other hand, all these cases are possible for the q_{HL} direction except for the case of phase changes in both material A and B due to the temperature inequality order. Through multiple steps to simultaneously solve the equation (2) for Fourier's law, we can firstly derive a relation of the phase change position in a certain material, and then obtain the magnitude of steady heat flux sequentially. The general solutions to all cases on both directions are summarized in Table I and II.

C. Criteria to determine phase situations

The criterion parameters are important since they are related to how many phase changes occur and in which material. Thus, they determine which heat flux relation for q_{LH} in Table I or for q_{HL} in Table II is appropriate. These criterion parameters are defined by both boundary temperatures (T_H and T_L) and thermophysical properties of A and B. The following dimensionless temperatures

$$\theta_A = \frac{T_A^* - T_L}{T_H - T_A^*} \quad \text{and} \quad \theta_B = \frac{T_B^* - T_L}{T_H - T_B^*} \tag{3}$$

are introduced as representative parameters for thermal condition effects on judging the cases. The criterion for each direction is separately proposed since the possible number of phase changes is different. There are two criterion relations for each material for the q_{LH} direction. In order for a phase change to occur in material A, the temperature at the junction point between materials A and B should be larger than the phase change temperature T_A^*. Starting from the inequality condition, we can obtain a relation that $1/\theta_A > R_{LH,A}$, where dimensionless $R_{LH,A}$ is

$$R_{LH,A} = \frac{(1 - k_{B,H}/k_{B,L})(k_{A,L} l_B + k_{B,L} l_A)}{l_A (k_{B,H} + k_{B,L} \theta_B)} + \frac{k_{A,L}}{k_{B,L}} \frac{l_B}{l_A} \tag{4}$$

Similarly, from a physical condition between T_b^* and junction temperature, we can derive a relation detailing the existence of material B that $\theta_B > R_{LH,B}$, where $R_{LH,B}$ is

$$R_{LH,B} = \frac{(1 - k_{A,L}/k_{A,H})(k_{A,H} l_B + k_{B,H} l_A)}{l_B (k_{A,L} + k_{A,H}/\theta_A)} + \frac{k_{B,H}}{k_{A,H}} \frac{l_A}{l_B} \tag{5}$$

The two criteria for q_{LH} independently determine the existence of phase change in material A and B, as summarized in Table I.
In the q_{HL} direction, one phase change can occur at most. From the same comparison, a criterion R_{HL} is found to be sufficient for determining whether or not the phase change for both materials exists. The detailed inequality conditions are summarized in Table II.

$$R_{HL} = \frac{k_{A,H}}{k_{B,L}} \frac{l_B}{l_A} \tag{6}$$

D. Adjustment method for extended conditions

The above criteria and the general solutions in Table I and II are valid only when the phase change temperatures are within boundaries $T_L \le T_A^* \le T_H$ and $T_L \le T_B^* \le T_H$. If T_A^* or T_B^* is outside these ranges, no phase change should arise. Should this be the case, the material can be assumed to possess a constant overall thermal conductivity. To adjust the situations with correct properties, we have to substitute $k_{A,H}$ for $k_{A,L}$ and/or $k_{B,L}$ for $k_{B,H}$ to the relations and criteria for the q_{LH} in Table I when $T_A^* < T_L$ and/or $T_B^* > T_H$, respectively. Likewise, when $T_A^* > T_H$ and/or $T_B^* < T_L$, the values of $k_{A,L}$ and/or $k_{B,H}$ for the q_{HL} are substituted for $k_{A,H}$ and/or $k_{B,L}$ in Table II, respectively. Another adjustment for the q_{HL} is additionally needed since R_{HL} is a single criterion for both materials, and mentioned in Table II. On the boundary of criteria, the solutions to the heat flux of both sides should be physically continuous and the continuity was validated.

III. CASE STUDY

A. Applied materials

Based on this general theory, we introduce a candidate material pair to show the potential thermal rectification effect of phase change heterojunctions. At room temperature or above, where most thermal diodes are used, low temperature thermal conductivities in the solid-state phase are higher than the high temperature thermal conductivities, such as polyethylene[25] (material A in the model). To maximize thermal rectification of the heterojunction, choosing a material with the opposite temperature trend can be a promising design for the other side. One candidate is metallic VO_2[24] (material B in the model). Indeed, the materials have the thermal conductivities like a step function,[24, 25] and have been used in literature.[21] The narrow transition temperature range hardly degrades the thermal rectification factor as enough thermal bias is applied.[22] The phase change temperatures and amplitude of thermal conductivity for both materials are tunable, either by doping,[24] geometric factor,[25] or stress.[25] For this work, we used the thermal conductivity data of the polyethylene by large-scale molecular dynamics simulations and the metallic VO_2[24] by experimental measurements on a suspended device. Both temperature-dependent thermal conductivities show that the shapes are good approximation of step functions even at the length scale of <100 nm. Even though VO_2 exhibits a hysteresis effect in heating and cooling processes, the general theory can cover the both heat flux based on different properties from the hysteresis. Since our theory is general and we wish to test an example with more varieties of phase change states, we assume VO_2 has a higher value of virtual representative phase change temperature as T_B^*=340 K than the polyethylene with T_A^*=320 K. Otherwise, we do not optimize other material properties (such as thermal conductivity ratio across phase change temperature) to achieve best performance instead we keep them the same as literature values,[24, 25] as summarized in Table III.

B. General theory results

Figure 2 shows the thermal rectification factor dependent on thermal bias. The interface positions of phase change in both materials move with respect to the change of temperature T_H, as the temperature T_L at the other end is fixed. The moving phase change interfaces in both materials are responsible for the various cases of thermal rectification. In the given conditions, seven distinct regions with different slopes of the thermal rectification factor are observed. All of which are derived from different phase change states. Two representative states, yielding different thermal rectification trends, are described as schematics in the insets. The thermal bias determines the phase changes, and thus defines the overall thermal conductivity and heat flux in each state and direction. The changing overall thermal conductivities are the underlying phenomenology behind thermal rectification.

At the flat regions in Fig. 2, we note that there is no phase change in either direction or material. The junction with two materials possessing the thermally opposite phase change trends is expected to perform high thermal rectification. In this case, the solid-state junction using the phase change materials shows a maximal thermal rectification factor of 80%, with a great potential to achieve a higher thermal rectification compared to the concept with an asymmetric shape of a material such as the 7% of a carbon nanotube[6] and 28% of VO_2.[8] Furthermore, as the concept developed in this work is based on bulk properties, the solid-state thermal device can be scaled up significantly more easily in comparison to nanostructures in the literature.

The general theory presented above offers a physical interpretation of thermal rectification, thus directly examining the contribution of each parameter to the thermal rectification factor and the relationship among these parameters. As investigating to optimize the thermal rectification factor according to geometric characteristics, we can recognize the thermal rectification of the junction depends on the length ratio l_A/l_B of the materials, not on the length itself. As shown in Fig. 3 which presents the thermal rectification factor obtained by the length ratio and thermal bias, the length ratio l_A/l_B, as a design parameter, is a critical parameter to determine the trend of thermal rectification factor, as well as its maximal value. Furthermore, under particular conditions such as the black line of $l_A/l_B = 2^3$, we can observe more than one local maximum. The result with plural optimization points represents that the solid-state junction is dominated by the complex phase change scenarios and this general theory is able to provide a design guide for thermal devices from testable predictions.

IV. Global optimal solution

This general theory works as a powerful and convenient tool to understand the physics of different cases of phase change in the heterojunction and the theoretical limitations on the performance of such a thermal diode. The general theory shows that the phase change temperature as well as the length ratio are two knobs to tune the thermal rectification factor. In order to examine the maximum potential rectification behavior possible across the heterojunction, we study the effect that changing the phase change temperature in each material has. In the following analysis, T^*_{VO2} is considered as a tuning parameter while $T^*_{Polyethylene}$ is fixed as 320 K and the generality of $T^*_A < T^*_B$ should be kept by choosing VO_2 as material A at the cases of $T^*_{VO2} < T^*_{Polyethylene}$. Figure 4 presents the dependence of the thermal rectification factor with respect to T^*_{VO2} for three different length ratios. The black dashed line in Fig. 4 refers to the condition where VO_2 has the same phase change temperature as polyethylene (i.e. 320 K). Two noticeable features emerge from this analysis, which we discuss below.

Feature one is that the optimal thermal rectification factor appears across a plateau region (and not at one particular point). The area inside the black solid line (the plateau region) has the same value of γ as a local maximum across the entire area. Basically, the highest possible γ available from the heterojunction, occurs when both materials are in their most thermally conductive phase in one direction and in their lowest thermally conductive phase in the other direction. However, as a practical matter, this limiting case seldom occurs in real systems, so, in general, it is important to examine the case where the local maximum γ predominates – this is where only one material is exhibiting a phase change interface in both directions. In this circumstance, the plateau regions confirm that the thermal rectification maxima are robust to small thermal perturbations from the ideal case. In more detail, when we check the phase change states of the plateau regions, there is only one phase change in both heat flux directions in the same material (in the VO_2 material at the length ratio conditions of Fig. 4(a) and (b), and in the polyethylene material at the condition of Fig. 4(c)).

We can derive the mathematical solution of γ for each region from the general theory summarized in Table I and II. When the phase change occurs only in material A (as is the case in Fig. 4 (c) which has a large length ratio l_A/l_B), the heat flux of each direction can be calculated as

$$q_{LH} = \frac{k_{B,H}\left\{k_{A,H}(T_H - T_A^*) + k_{A,L}(T_A^* - T_L)\right\}}{k_{A,H}l_B + k_{B,H}l_A} \tag{7}$$

$$q_{HL} = \frac{k_{B,L}\left\{k_{A,H}(T_H - T_A^*) + k_{A,L}(T_A^* - T_L)\right\}}{k_{A,L}l_B + k_{B,L}l_A} \tag{8}$$

At conditions that cause higher heat flux in the q_{LH} direction, the solution of γ in the case of a phase change in material A in both directions can be derived by inserting Eq. (7) and (8) into Eq. (1) as follows.

$$\gamma = \left(\frac{k_{A,L}}{k_{B,L}} + \frac{l_A}{l_B}\right) \Big/ \left(\frac{k_{A,H}}{k_{B,H}} + \frac{l_A}{l_B}\right) - 1 \tag{9}$$

Additionally, the solution of γ with a phase change in material B can be presented as

$$\gamma = \left(1 + \frac{k_{B,H}}{k_{A,H}}\frac{l_A}{l_B}\right) \Big/ \left(1 + \frac{k_{B,L}}{k_{A,L}}\frac{l_A}{l_B}\right) - 1 \tag{10}$$

Both equations are possible solutions for maximum γ, expressed as an independent relation of the thermal bias (T_H and T_L) and the phase change temperatures (T_A^* and T_B^*). It means that the change in overall thermal conductivity for both directions is maintained at a certain rate according to the thermal bias, even though the phase change interface is moving. Thus, the optimal plateau regions, which share an identical thermal rectification factor, occur due to the independency of the thermal rectification on the axis variables, the thermal bias and T^*_{VO2}.

The second feature worth noting arises that the thermal bias range satisfying the local optimal γ is the widest when the phase change temperatures of the two materials are identical, i.e. at the condition on the black dashed line in Fig. 4. As the phase change temperatures of two materials approach the same value, the possibility of the state with two phase changes in the q_{LH} direction disappears. The more phase change interface disturbs to actualize the higher thermal rectification from the appropriate thermally conductive phase for each heat flux direction. The state with only one phase change can utilize the proper phase of at least the other material which

a phase change does not occur, in contrast to the state with two phase changes. The reduced possibility of the additional phase change widens the thermal bias condition for the local maximum γ.

By leveraging the tunability of the phase change temperature, a solid-state junction consisting of two materials with an identical phase change temperature is the most promising case. Below, we examine the theoretical maximum thermal rectification factor in this case. One additional optimization parameter for this solid-state heterojunction is the ratio of the lengths of each segment of material, l_A/l_B. Figure 5 shows the maximal thermal rectification factor γ_{max} of the heterojunction at each length ratio condition. The results of γ_{max} corresponds to the mathematical solutions from Eq. (9) or Eq. (10), as expected from the above analysis. A global optimization value is obtainable from the intersection of the two equations. To achieve the global maximal performance of the heterojunction, the length ratio should satisfy the following relation of l_A/l_B.

$$l_A/l_B = \sqrt{\frac{k_{A,L}}{k_{B,L}}\frac{k_{A,H}}{k_{B,H}}} \tag{11}$$

Then, as the optimized length ratio inserts into Eq. (9) or Eq. (10), the equations result in the identical thermal rectification factor of

$$\gamma_{\max} = \sqrt{\frac{k_{A,L}}{k_{A,H}}\frac{k_{B,H}}{k_{B,L}}} - 1 \tag{12}$$

The theoretical maximum solution is based on the geometric mean of the thermal conductivity ratio of the two materials. The relation with the thermal conductivity ratio is consistent with our initial intuition of selecting polyethylene as material A ($k_{A,L}>k_{A,H}$) and VO_2 ($k_{B,L}<k_{B,H}$) as material B to achieve an effect of thermal rectification in this case study. The maximum solution shows there is no limit ceiling for the thermal rectification in this design. A phase change material with one phase change temperature makes two separate phases. Thus, two materials in the junction design are sufficient number to realize the effect of thermal rectification. Additionally, we are able to check that the length ratio for the high thermal rectification is dependent on the ratio of the general thermal conductivity between two phase change materials.

Upon close inspection of this condition of the length ratio for the theoretical maximum, a plateau region according to thermal bias does not appear, in other words, the optimum γ_{max} is observed at a specific thermal bias condition. The phase change temperature is located at the junction interface in both directions. Without any phase change in both materials, the heterojunction can be operated only with low thermal conductivities of both materials in one direction and high thermal conductivities in the opposite direction. As presented in Fig. 5, the heterojunction with the two materials has a theoretical potential to present the γ_{max} of over 140%. Although based on optimal phase change temperatures of materials and a specific thermal bias condition, the theoretical maximum value suggests the guidance for design and material selection, and clarifies the possibility of the heterojunction as a thermal rectifier with an outstanding thermal rectification factor.

V. CONCLUSION

In summary, we discussed a general theory for calculating thermal rectification of a solid-state junction comprised of two phase change materials. This provides a comprehensive analysis, considering whether phase changes happen in either (or both) of two material heterojunctions, was detailed. The analysis on a heterojunction by the general theory showed a possibility for obtaining a high thermal rectification. With a further analysis based on the tunable phase change materials, the general theory suggests the theoretical maximal thermal rectification factor from an optimization of design and thermal bias conditions. We believe the methodology in this work provides an effective way to explore the application of thermal rectification to a nonlinear thermal device.

ACKNOWLEDGMENTS

The work at the Molecular Foundry was supported by the Office of Science, Office of Basic Energy Sciences, at the U.S. Department of Energy (DOE), Contract No. DE-AC02-05CH11231. H. Kang gratefully acknowledges a financial support from Kwanjeong Educational Foundation. We are indebted to M. P. Gordon and W. Lee for critical reading of the manuscript.

REFERENCES

1. N. Li, J. Ren, L. Wang, G. Zhang, P. Hänggi and B. Li, Colloquium: Phononics: Manipulating heat flow with electronic analogs and beyond, Rev. Mod. Phys. **84**, 1045 (2012).
2. N. Yang, N. Li, L. Wang and B. Li, Thermal rectification and negative differential thermal resistance in lattices with mass gradient, Phys. Rev. B **76**, 020301 (2007).
3. M. Peyrard, The design of a thermal rectifier, Europhys. Lett. **76**, 49 (2006).
4. N. A. Roberts and D. Walker, A review of thermal rectification observations and models in solid materials, Int. J. Therm. Sci. **50**, 648 (2011).
5. Y. Wang, A. Vallabhaneni, J. Hu, B. Qiu, Y. P. Chen and X. Ruan, Phonon lateral confinement enables thermal rectification in asymmetric single-material nanostructures, Nano Lett. **14**, 592 (2014).
6. C. Chang, D. Okawa, A. Majumdar and A. Zettl, Solid-state thermal rectifier, Science **314**, 1121 (2006).
7. B. V. Budaev and D. B. Bogy, Thermal rectification in inhomogeneous nanotubes, Appl. Phys. Lett. **109**, 231905 (2016).
8. J. Zhu, K. Hippalgaonkar, S. Shen, K. Wang, Y. Abate, S. Lee, J. Wu, X. Yin, A. Majumdar and X. Zhang, Temperature-gated thermal rectifier for active heat flow control, Nano Lett. **14**, 4867 (2014).
9. T. Zhang and T. Luo, Giant thermal rectification from polyethylene nanofiber thermal diodes, Small **11**, 4657 (2015).
10. H. Wang, S. Hu, K. Takahashi, X. Zhang, H. Takamatsu and J. Chen, Experimental study of thermal rectification in suspended monolayer graphene, Nat. Commun. **8**, 15843 (2017).
11. R. Dettori, C. Melis, R. Rurali and L. Colombo, Thermal rectification in silicon by a graded distribution of defects, J. Appl. Phys. **119**, 215102 (2016).
12. Z. Chen, C. Wong, S. Lubner, S. Yee, J. Miller, W. Jang, C. Hardin, A. Fong, J. E. Garay and C. Dames, A photon thermal diode, Nat. Commun. **5** (2014).
13. P. Ben-Abdallah and S.-A. Biehs, Phase-change radiative thermal diode, Appl. Phys. Lett. **103**, 191907 (2013).
14. A. Ghanekar, J. Ji and Y. Zheng, High-rectification near-field thermal diode using phase change periodic nanostructure, Appl. Phys. Lett. **109**, 123106 (2016).
15. C. Dames, Solid-state thermal rectification with existing bulk materials, J. Heat Transf. **131**, 061301 (2009).
16. D. M. Leitner, Thermal boundary conductance and thermal rectification in molecules, J. Phys. Chem. B **117**, 12820 (2013).
17. W. Kobayashi, Y. Teraoka and I. Terasaki, An oxide thermal rectifier, Appl. Phys. Lett. **95**, 171905 (2009).
18. D. Sawaki, W. Kobayashi, Y. Moritomo and I. Terasaki, Thermal rectification in bulk materials with asymmetric shape, Appl. Phys. Lett. **98**, 081915 (2011).
19. W. Kobayashi, D. Sawaki, T. Omura, T. Katsufuji, Y. Moritomo and I. Terasaki, Thermal rectification in the vicinity of a structural phase transition, Appl. Phys. Express **5**, 027302 (2012).
20. R. Chen, Y. Cui, H. Tian, R. Yao, Z. Liu, Y. Shu, C. Li, Y. Yang, T. Ren and G. Zhang, Controllable thermal rectification realized in binary phase change composites, Sci. Rep. **5**, 8884 (2015).
21. A. L. Cottrill and M. S. Strano, Analysis of thermal diodes enabled by junctions of phase change materials, Adv. Energy Mater. **5**, 1500921 (2015).
22. A. L. Cottrill, S. Wang, A. T. Liu, W. J. Wang and M. S. Strano, Dual phase change thermal diodes for enhanced rectification ratios: Theory and experiment, Adv. Energy Mater **8**, 1702692 (2018).
23. J. Ordonez-Miranda, J. M. Hill, K. Joulain, Y. Ezzahri and J. Drevillon, Conductive thermal diode based on the thermal hysteresis of VO2 and nitinol, J. Appl. Phys. **123**, 085102 (2018).
24. S. Lee, K. Hippalgaonkar, F. Yang, J. Hong, C. Ko, J. Suh, K. Liu, K. Wang, J. J. Urban and X. Zhang, Anomalously low electronic thermal conductivity in metallic vanadium dioxide, Science **355**, 371 (2017).

25. T. Zhang and T. Luo, High-contrast, reversible thermal conductivity regulation utilizing the phase transition of polyethylene nanofibers, ACS nano **7**, 7592 (2013).
26. D.-W. Oh, C. Ko, S. Ramanathan and D. G. Cahill, Thermal conductivity and dynamic heat capacity across the metal-insulator transition in thin film VO_2, Appl. Phys. Lett. **96**, 151906 (2010).
27. M. D. Losego, L. Moh, K. A. Arpin, D. G. Cahill and P. V. Braun, Interfacial thermal conductance in spun-cast polymer films and polymer brushes, Appl. Phys. Lett. **97**, 011908 (2010).
28. D. G. Cahill, W. K. Ford, K. E. Goodson, G. D. Mahan, A. Majumdar, H. J. Maris, R. Merlin and S. R. Phillpot, Nanoscale thermal transport, J. Appl. Phys. **93**, 793 (2003).
29. M. D. Losego, M. E. Grady, N. R. Sottos, D. G. Cahill and P. V. Braun, Effects of chemical bonding on heat transport across interfaces, Nat. Mater. **11**, 502 (2012).
30. S. Majumdar, J. A. Sierra-Suarez, S. N. Schiffres, W.-L. Ong, C. F. Higgs III, A. J. McGaughey and J. A. Malen, Vibrational mismatch of metal leads controls thermal conductance of self-assembled monolayer junctions, Nano Lett. **15**, 2985 (2015).
31. H. Acharya, N. J. Mozdzierz, P. Keblinski and S. Garde, How chemistry, nanoscale roughness, and the direction of heat flow affect thermal conductance of solid–water interfaces, Ind. Eng. Chem. Res. **51**, 1767 (2011).
32. H. D. Pandey and D. M. Leitner, Influence of thermalization on thermal conduction through molecular junctions: Computational study of PEG oligomers, J. Chem. Phys. **147**, 084701 (2017).

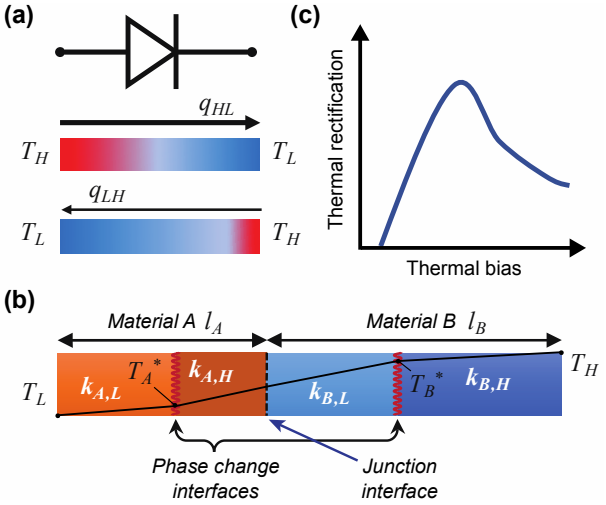

FIG. 1 Basic concept of thermal rectification and the heterojunction using two phase change materials in series. (a) Analogous to the electrical diode, the thermal rectifier transmits heat more easily in one direction than in the reverse direction. The subscript HL and LH indicate the direction of heat flux, from high (H) to low (L) temperature, or vice versa. (b) Schematic geometry of the suggested junction. The terminologies and symbols introduced here will be used throughout the paper. The black line represents the temperature profile within the structure when phase changes exist in both A and B materials (c) Schematic of expected thermal rectification with respect to thermal bias via phase change materials.

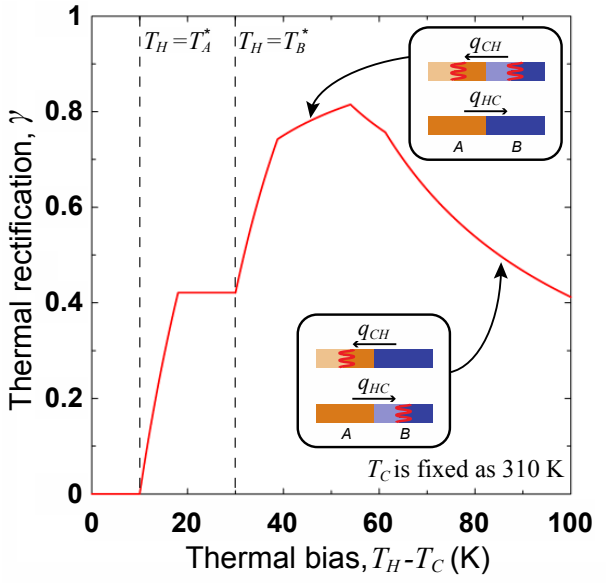

FIG. 2 Thermal bias dependent thermal rectification via a heterojunction between polyethylene (material A)[25] and tungsten doped VO_2 (material B)[24] as detailed in Table III. Regimes with different slopes represent different combinations of phase change states between the two materials Two representative states yielding different thermal rectification trends are detailed in the inserts.

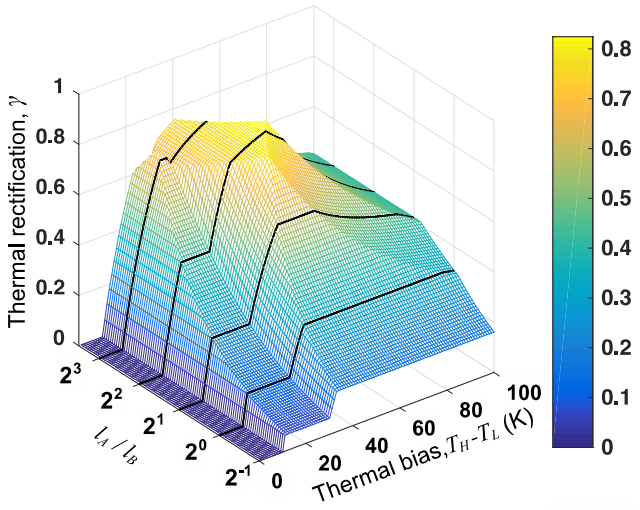

FIG. 3 Optimal thermal rectification with respect to a selected design parameter, the length ratio l_A/l_B. 3D mesh graph shows the existence of local and general optimization points for thermal rectification. (Other parameters are detailed in Table III)

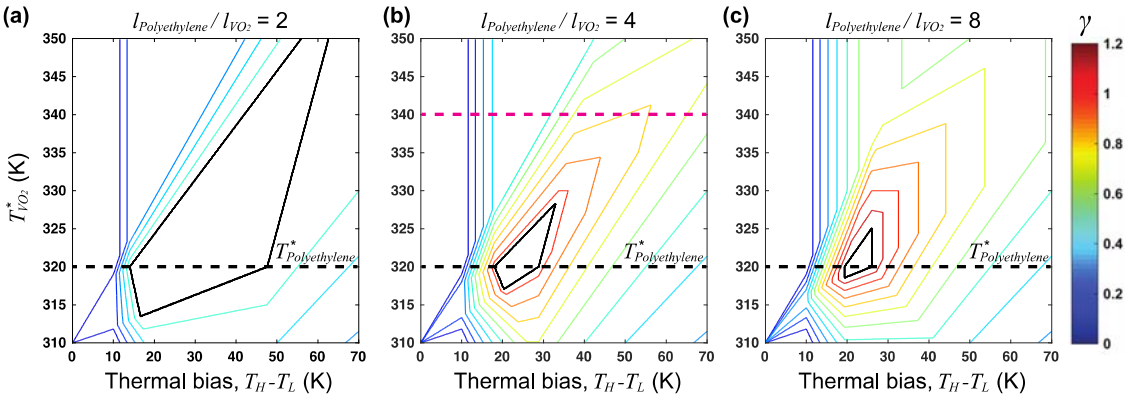

FIG. 4 Optimal thermal rectification with respect to phase change temperature at the defined length ratio, (a) $l_{VO_2}/l_{Polyethylene} = 2$, (b) $l_{VO_2}/l_{Polyethylene} = 4$ and (c) $l_{VO_2}/l_{Polyethylene} = 8$. The area inside the black line in each figure has the same thermal rectification factor γ and the maximum value of γ. The black dashed lines mean the condition the VO_2 has the same phase change temperature with the polyethylene as 320 K. The magenta dashed line in (b) corresponds to the condition of the case study at Fig. 2. (Other parameters are detailed in Table III)

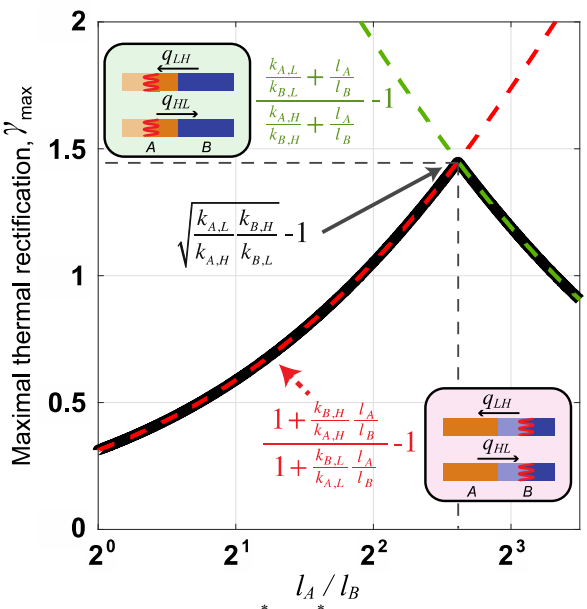

FIG. 5 Maximal thermal rectification γ_{max} with $T_A^* = T_B^*$ condition at each length ratio. The green line is the solution of γ for the case of a phase change in material A in both directions and the red line is the solution for that in material B. The global maximal rectification is observed at the intersection between the two solutions. The theoretical maximal rectification is based on the geometric mean of the thermal conductivity ratio of the two materials as expressed as $\sqrt{\frac{k_{A,L}}{k_{A,H}} \frac{k_{B,H}}{k_{B,L}}} - 1$ with the optimized length ratio of $\frac{l_A}{l_B} = \sqrt{\frac{k_{A,L}}{k_{B,L}} \frac{k_{A,H}}{k_{B,H}}}$. (Other parameters are detailed in Table III)

Table I. Heat flux relations for q_{LH} with corresponding criteria. The criteria on columns and rows independently determine the existence of phase change in material A and B, respectively.

$q_{LH}=$	Phase change in A: $1/\theta_A > R_{LH,A}$	No phase change in A: $1/\theta_A \leq R_{LH,A}$
Phase change in B: $\theta_B > R_{LH,B}$	$\frac{\left\{k_{A,H}(T_H - T_A^*) + k_{A,L}(T_A^* - T_L)\right\}\left\{k_{B,H}(T_H - T_B^*) + k_{B,L}(T_B^* - T_L)\right\} + (k_{A,H} - k_{A,L})(k_{B,H} - k_{B,L})(T_H - T_B^*)(T_A^* - T_L)}{(T_H - T_L)(k_{A,H}l_B + k_{B,L}l_A)}$	$\frac{k_{A,L}\left\{k_{B,H}(T_H - T_B^*) + k_{B,L}(T_B^* - T_L)\right\}}{k_{A,L}l_B + k_{B,L}l_A}$
No phase change in B: $\theta_B \leq R_{LH,B}$	$\frac{k_{B,H}\left\{k_{A,H}(T_H - T_A^*) + k_{A,L}(T_A^* - T_L)\right\}}{k_{A,H}l_B + k_{B,H}l_A}$	$\frac{k_{A,L}k_{B,H}(T_H - T_L)}{k_{A,L}l_B + k_{B,H}l_A}$

Table II. Heat flux relations for q_{HL} with corresponding criteria. The relation on the second column is about the state of the absence of phase change in both materials.

	Phase change in A: $R_{HL} < \theta_A$	No change: $\theta_A \le R_{HL} \le \theta_B$ †	Phase change in B: θ_B † $< R_{HL}$
$q_{HL} =$	$\dfrac{k_{B,L}\left\{k_{A,H}(T_H - T_A^*) + k_{A,L}(T_A^* - T_L)\right\}}{k_{A,L}l_B + k_{B,L}l_A}$	$\dfrac{k_{A,H}k_{B,L}(T_H - T_L)}{k_{A,H}l_B + k_{B,L}l_A}$	$\dfrac{k_{A,H}\left\{k_{B,H}(T_H - T_B^*) + k_{B,L}(T_B^* - T_L)\right\}}{k_{A,H}l_B + k_{B,H}l_A}$

† when $\theta_B < 0$, there is no phase change in both materials. It is equivalent to assume θ_B as very large number

Table III. Material properties used for the calculation in this manuscript for polyethylene (material A)[25] and tungsten doped VO_2 (material B).[24]

T_A^* (K)	T_B^* (K)	$k_{A,L}$ (W/mK)	$k_{A,H}$ (W/mK)	$k_{B,L}$ (W/mK)	$k_{B,H}$ (W/mK)	l_A/l_B (-)
320	340 †	30	10	2	4	4

† The value of T_B^* is virtual